Archives of Materials Science and Engineering

Volume 43
Issue 2
June 2010
Pages 94-100

International Scientific Journal published monthly by the World Academy of Materials and Manufacturing Engineering

Mechanical approach of PP/MMT polymer nanocomposite

L.A. Dobrzański [a,*], M. Bilewicz [a], J.C. Viana [b]

[a] Division of Materials Processing Technology, Management and Computer Techniques in Materials Science, Institute of Engineering Materials and Biomaterials, Silesian University of Technology, ul. Konarskiego 18a, 44-100 Gliwice, Poland

[b] Institute for Polymers and Composites, Department of Polymer Engineering, University of Minho, 4800-058 Guimarães, Portugal

* Corresponding author: E-mail address: leszek.dobrzanski@polsl.pl

Received 17.02.2010; published in revised form 01.06.2010

ABSTRACT

Purpose: Paper summarizes and focus on investigation of PP/MMT nanocomposite in mechanical and statistical approach.

Design/methodology/approach: Research has been performed basing on design of experiment.

Findings: Considerable predominance of PP + nanoclay mixture in the increment of absorption of energy is found; Level of absorbed energy, required to break the specimens during fracture test is two times higher after structure reinforcement by nanoparticles.

Research limitations/implications: Non-conventional injection moulding gives us possibility to control orientation level and develop morphology and it is limited due to non-conventional injection system limitation (pressure, time etc).

Practical implications: PP/MMT nanocomposites are the materials with promising future wide range of application also in the specific branches like car and aircraft industries.

Originality/value: Nanocomposites obtained in experiment obtaining allow to achieve shish-kebab structure, reinforce skin/core structure and improve mechanical behaviour

Keywords: Engineering materials; MMT; Polymer nanocomposites; Polymer processing

Reference to this paper should be given in the following way:

L.A. Dobrzański, M. Bilewicz, J.C. Viana, Mechanical approach of PP/MMT polymer nanocomposite, Archives of Materials Science and Engineering 43/2 (2010) 94-100.

MATERIALS MANUFACTURING AND PROCESSING

1. Introduction

Features like mechanical properties and morphology of injection moulded composites, strongly depend on thermomechanical processing variables [1]. It is noteworthy that by compounding and processing (thermally, mechanically) of different polymers and reinforcements can be explored diversity of morphologies. The most fundamental and important aim in the polymer composites is control of the morphology [2-7]. This control significantly influences properties of materials. Change of the structure on molecular or macroscopic level may improve dramatically mechanical properties, e.g. modulus, stiffness and impact strength [8-12] as well toughness and flexural modulus. Microscopic observations has been done for better understanding of conformity between:

i) processing conditions and morphology,
ii) mechanical properties and morphology.

© Copyright by International OCSCO World Press. All rights reserved. 2010

In the polymer blends meaningful point is miscibility which depends on the balance of small enthalpic and non-configurational entropic effects [2]. Nevertheless better characteristics can be obtained, in many cases, just by using heterogeneous blends with partial miscibility [13].

The immiscibility prevails while miscibility is limited to a specific condition statement. Majority of polymers form blends, which require compatibilization. Among many techniques of compatibilization as reactive compounding or mechano-chemical blending we can distinguish addition of a small quantity of third component, miscible with both phases. In this investigation polypropylene grafted maleic anhydride (table 1) has been used as compatybilizer in the ratio of 3 wt% of major polymer in the blend [14,15]. Silicates like montmorillonite have been used as reinforcing materials for polymer composites owing to their high aspect ratio and unique intercalation/exfoliation characteristics. Nanocomposite of polymer-montmorillonite was obtained by widely used formation method – melt compounding [16] and inclusion just before injection. The clay's particles are diffused between particles of polymer matrix. Normally the evident crystallinity increases with filler content and becomes asymptotic for more than 2% filler [17, 18]. In the experiment has been used 3 wt% of nano-sized layered silicates based on montmorillonite to obtain nanocomposites, which possess apparent change of mechanical properties and represents wide field of research and applications since 1989 [19,20]. Receiving shish-kebab structure, which can be obtained by non-conventional injection moulding technique was considered in the experiment. An interesting fibre-like morphology, which is crystallized from a solution by stirring during cooling, was first observed by Pennings & Kiel [21]. Oriented species play a prominent role in formation of stretched sections, where shish originates. Conventional injection moulding process consists on injection of thoroughly plasticized melt of plastic material into the clamped mold, where the end-product is formed.

The target of this work was to investigate the mechanical behaviour improvements of polymer-polymer composites injected by non-conventional technique, which allows adjusting of processing settings by, among other things, controlling shear rate, injection speed and melt temperature. Application of non-conventional injection moulding gives us possibility to control orientation level, develop morphology, also by obtaining shish-kebab structure, reinforce skin/core structure and improve mechanical behaviour. The future work should include application of neural network, which can predict behaviour of structure and thus mechanical response.

2. Experimental

2.1. Materials

In the experiment three, differently aimed materials have been used. Polypropylene as inexpensive, commercial and worldwidely available material was used as matrix in experiment. Nanoclay (MMT) – high purity layered silicates based on montmorillonite, strongly influencing structure of composites, was distributed inside material as reinforcing phase. Better compatibilization was expected to obtain by addition of PP grafted with maleic anhydride (MAP). Materials' specifications (Table 1) and mutual proportions (Table 2) are described below.

2.2. Specimen preparation

Blending of PP/MAP and PP/Nanoclay at fixed ratio (97/3 wt/%) was conducted by mixing dried materials in the barrel at room temperature and rotor speed 60 rpm. Composite preparation has been used just before locating in the moulding machine feeder. Injection moulding process for all specimens has been done on the Ferromatik Milacron injection moulding machine model K-85 by using conventional and non-conventional SCORIM technique. Non-conventional technique has been used to induce multilayer structure by high shear rate treatment of the melt. The blends composition was designated in the special manner. After compounding, the blends were conventionally injection moulded into standard rectangular bar with dimensions 130 mm x 13 mm x 8 mm. Temperature settings of five barrel zones of the machine was 240/230/220/210/140 ºC from nozzle to hopper. Mould temperature was 30 ºC. Injection flow rate (10 mm/s), holding pressure (50 bar) and cooling time (30 s) were kept constant for all specimens.

The same blends composition was used subsequently in the non-conventional injection moulding technique performed on specially adopted injection machine (Fig. 1). This technique consists on the handling of the melt polymer, which is provided through two hot-runner channels, and originate high shear rate by using various movements of external pistons to obtain outer highly oriented multi-layers and a less oriented inner core. Pistons' movements were set in 2 modes. Initial mode called out-of-phase consists on alternating extension and retraction of the melt in the mould cavity. During this mode is created structure in the rectangular shape bar, composed of two phases - skin and core, forming miscellaneous morphology. Second mode represents hydrostatic pressure throughout its pressure is kept on constant level. For experiment has been used injection pressure of 150bar. Each set-up is finished by this mode. There is also possibility to use in-phase mode for compressing and extracting. In the experiment have been used mode out-of-phase and hydrostatic pressure.

Fig. 1. Injection molding machine with special mold , remotely operated

Table 1.
Materials used in experiment

Materials	Brand	Supplier	Characteristics
PP	Moplen HP 501M	Basell Plasticos, Lda	density: 0.9 g/cm^3, melt temp: 200ºC
MMT	Nanofil 5	Süd-Chemie	density: 1.8 g/cm^3 melt temp: >390ºC particle size: 1x300x300 nm
MAP	Licomont AR 504	Clariant GmbH	density: 0.91 g/cm^3, melt temp: 156ºC

Table 2.
Injection moulding processing variables for CIM and N-CIM

Run	Tmelt (Tm) [ºC]	Stroke time (St) [s]	Stroke number (Ns)	Shearing time [s]
CIM Injection moulding processing variables				
1	1 (240ºC)	-	-	1
2	2 (280ºC)	-	-	1
N-CIM Injection moulding processing variables				
1	1 (240ºC)	1 (1s)	1 (3)	4
2	1	2 (3s)	1	10
3	1	1	2 (12)	13
4	1	2	2	37
5	2 (280ºC)	1	1	4
6	2	2	1	10
7	2	1	2	13
8	2	2	2	37

Table 3.
Injection moulding processing variables for CIM and N-CIM

Moulding condition		neat PP			PP/MAP			PP/Nanoclay		
		E [MPa]	K_I $\left[\frac{(MPa\cdot m)}{2}\right]$	G_{1C} [J]	E [MPa]	K_I $\left[\frac{(MPa\cdot m)}{2}\right]$	G_{1C} [J]	E [MPa]	K_I $\left[\frac{(MPa\cdot m)}{2}\right]$	G_{1C} [J]
N-CIM	1	1322	8.946	0.009	1208	7.927	0.018	1283	7.145	0.029
	2	1376	7.935	0.014	1259	7.249	0.016	1213	7.227	0.048
	3	1309	8.262	0.016	1244	7.932	0.016	1257	7.376	0.027
	4	1392	8.403	0.022	1287	7.742	0.020	1247	7.161	0.035
	5	1236	7.806	0.010	1194	6.951	0.014	1209	7.018	0.035
	6	1214	7.180	0.017	1241	7.738	0.010	1220	7.854	0.026
	7	1266	7.268	0.010	1217	7.997	0.014	1244	7.530	0.030
	8	1251	7.612	0.019	1280	7.732	0.016	1274	7.599	0.033
	Var(%)	14.6	24.59	1.09	7.78	15.05	1.01	6.12	11.91	0.83
CIM	1	1128	7.514	0.020	1235	7.261	0.017	1314	6.726	0.025
	2	1352	8.154	0.014	1247	7.192	0.012	1266	7.149	0.030
	Var(%)	19.85	8.52	0.43	0.97	0.96	0.38	3.8	6.29	0.21

E – flexural modulus, K_I – fracture toughness, G_{1C} – fracture energy at break point, $Var\,(\%) = \frac{(\max - \min)}{\min} \times 100$

2.3. Mechanical testing

Universal testing machine type Instron 4505 was used for 3-point bending fracture test with crosshead speed 10mm/min (ASTM E399) and for flexural test with crosshead speed 2.8mm/min (ISO 178 -75). For fracture test has been used single edge notch bending geometry of the specimen with notch depth of 6.35mm. Notch has been machined on notch cutter type CEAST 6816 with the blade type 6530 and then sharpened by razor blade. Tests were following rules specified by the international standard norms. For proper calculation minimum five specimens were tested for each test. The average value and standard deviation have been calculated. All specimens were tested at 23 ºC.

2.4. Optical characterization - light polarized microscopy (PLM)

To obtain PLM photos, has been used Olympus Light Microscopy type BH2 with additional digital camera Olympus DP11, which includes imaging in the polarized light. Observations and layers counting have been computer-aided by measuring interactive program Quantimet 500C. Cross sections were chosen from the same regions from specimens and then carefully cut in order to obtain suitable surface quality for observation. Thin slices with thickness of 20 µm have been performed on the cut machine Microtom Anglia Scientific.

2.5. Processing set-up

Diverse injection moulding variables of conventional and non-conventional techniques have been used and they are described in this chapter. For all specimens in both conditions injection pressure has been 150 bar and kept constant, as well other parameters - holding pressure (50 bar), mold temperature (30ºC), cooling time (30 s), injection flow rate (15 mm/s). Changeable processing parameters were the melt temperature, the stroke time and the number of strokes. Set-up of these factors is following accordingly to 2-level Taguchi Orthogonal Array L8 carried out by using design of experiments. Settings for CIM, presented in the Table 2, contain in the last column time, when flow was under shear (injection time). Table 3 presents the processing variables for the 8 N-CIM runs and their limits of variation. Shear time has been counted as the total time of SCORIM movements and injection time (1 second, constant for all injections).

3. Results and discussion

3.1. Morphological approach

Primary point in discussion is the morphological study. Specimens have been observed in PLM in the aim to understanding the structure and recognizing the layers thickness and quantity. PLM photos are organized in accordance to statistical array (Table 2).

Core/sheared zone ratio has been counted by using detection techniques on image analysis program. Order of image analyzing steps is presented below (Fig. 2).

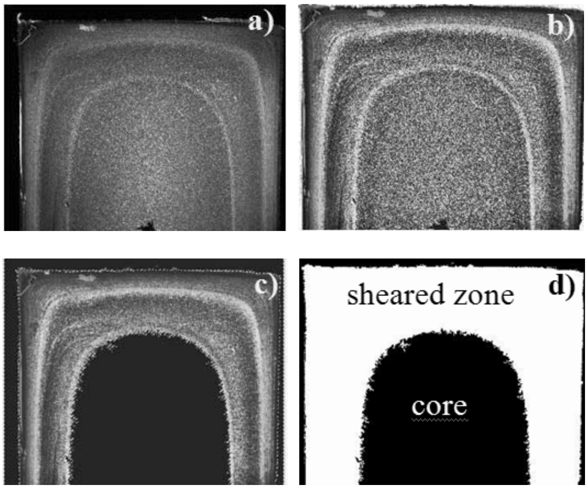

Fig. 2a. Order of computer aided image analysis and area calculations of PLM images of N-CIM a) direct image from PLM, b) contrast-brightness improvement, c) edge detection, d) mask overlapping with core in black and sheared zone in white color

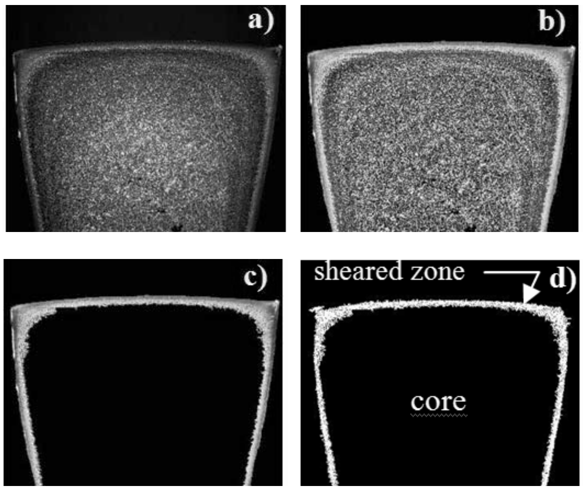

Fig. 2b. Order of computer aided image analysis and area calculations of PLM images of CIM a) direct image from PLM, b) contrast-brightness improvement, c) edge detection, d) mask overlapping with core in black and sheared zone in white color

General difference between CIM and N-CIM structures, presented on photos below, is the shrinkage. Cross section area of whole specimen obtained by CIM contains around 17% shrinkage, comparing to N-CIM. For both techniques has been used equal injection and holding pressure.

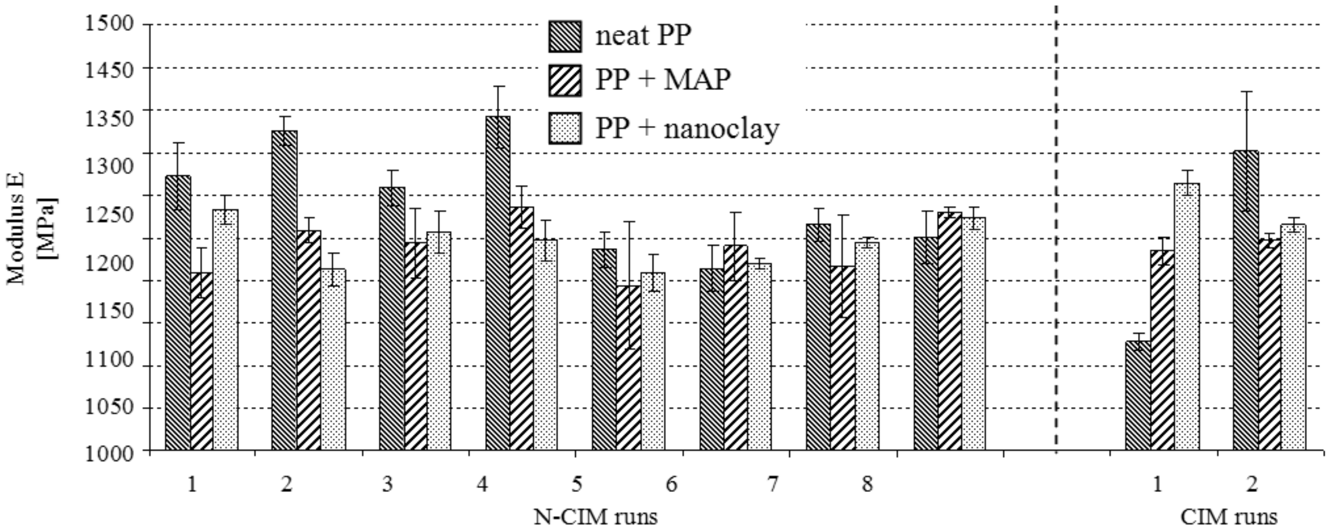

Fig. 3. Modulus of the materials' systems processed by both techniques

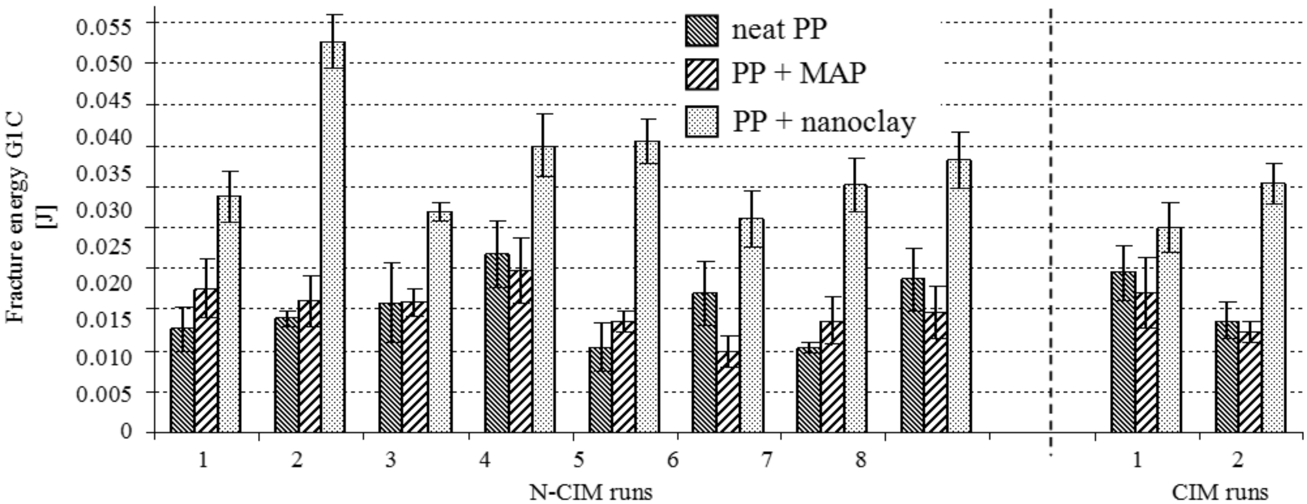

Fig. 4. Fracture energy of the materials' systems processed by both techniques

Reciprocation of SCORIM movements fulfills tightly mould capacity, not allowing material to shrink. Cross sections of CIM of PP specimens, visible in polarized light, present uniform appearance (Fig. 2). Core occupies the biggest area and simultaneously skin doesn't occur in more than one, thin layer. Higher stiffness, considered in the next chapter, has been obtained in the specimens, created under higher temperature processing (280ºC). Core contains approximately 10 times bigger area than skin for both temperatures. N-CIM core/sheared zone systems of PP, visible on the PLM images (Fig. 3), present higher diversification. Arrangement of photos, accordingly to shearing time, show increment of core/shear zone ratio accordingly to increment of shear time, however the highest run doesn't represent the maximal level of reinforcing.

3.2. Mechanical approach

The organization of mechanical results is presented in the following order: at first are discussed mechanical properties of the material systems. Then the mechanical properties of the moldings are classified according to the type of injection moulding technique and processing factors. Table 3 presents mechanical properties of the moldings for neat PP, PP/MAP and PP/Nanoclay obtained in non-conventional SCORIM technique and for comparison in conventional technique. Each run in the table corresponds to different settings of the changeable parameters during injection moulding process and cause various results of mechanical properties.

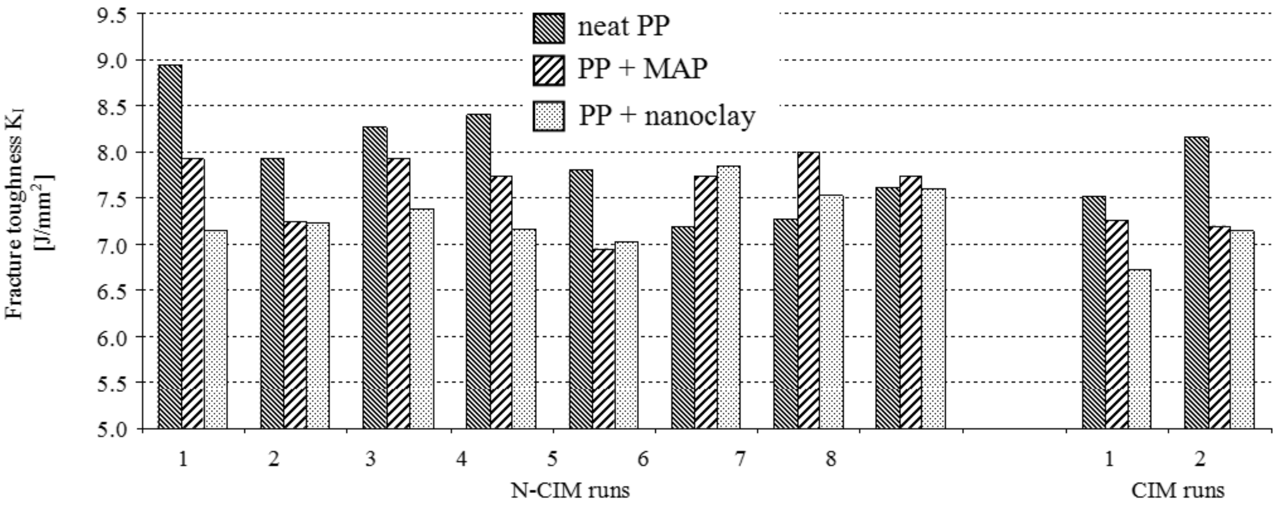

Fig. 5. Fracture toughness of the materials' systems processed by both techniques

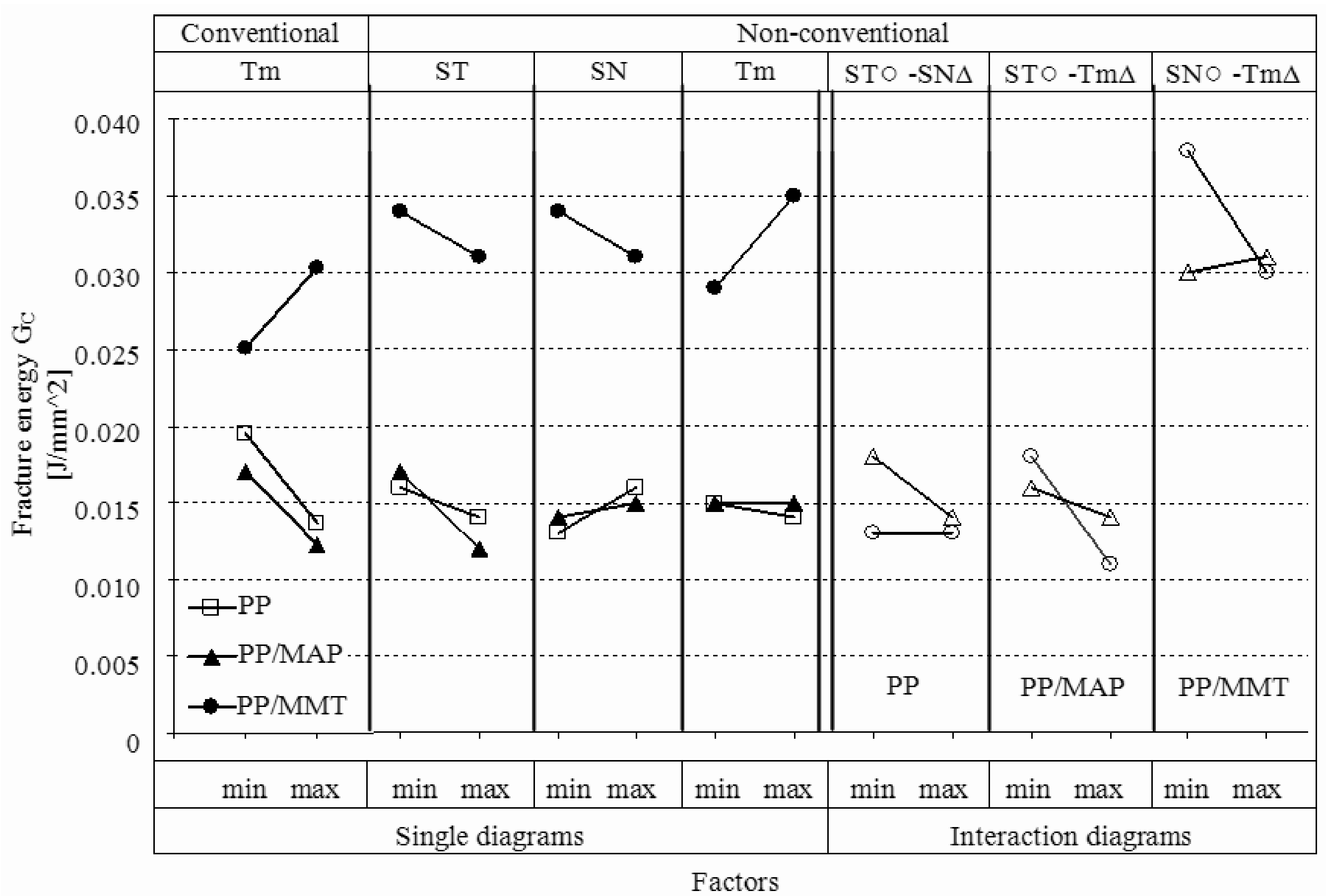

Fig. 6. Statement of the single and interaction diagrams of the factors, basing on the full DOE processing values, according to the Table 1, over the fracture energy G_{1C} of PP, PP/MAP and PP/MMT

SCORIM technique characterizes obtainment of skin-sheared zone-core structure. The outer area contains multilayer construction composed from layers and outside skin. Layers obtained during injection moulding process are oriented in accordance to flow direction of injected and solidifying melt in the cavity reinforce material systems. The general advantage of N-CIM is the structure development and thus higher mechanical resistance in comparison to conventional technique.

Comparing flexural modulus and fracture toughness results we can see advantage of SCORIM method to provide enhanced strength than conventional one (Figs. 3-5).

Considerable predominance of PP + nanoclay mixture in the increment of absorption of energy can be seen. Level of absorbed energy (Fig. 4), required to break the specimens during fracture test is two times higher in the case, when the nanoparticles are reinforcing structure of material. Internally located particles in the material system prolong the crack propagation and finally the break. Slalom-like crack propagation comes slower in the time by reason of bypassing parallel oriented lamella-like nanoclay tactoids.

The statistical calculations for influence of processing parameters over mechanical properties have been done. As is shown on the graph (Fig. 6) the biggest influence for PP originates from stroke number parameter and with its increment, increases adhesive energy G1C. Different behaviour is for PP + MAP, where G1C mainly depends from stroke time and simultaneously decreases with its increment. Most significant parameters controlling mechanical response in the PP + nanoclay is the interaction between stroke number and melt temperature and energy increases with their decrement and increment respectively.

References

[1] J.C. Viana, A.M. Cunha, N. Billon, The Tensile Behaviour of an Injection-Moulded Propylene-Ethylene, Polymer International 43 (1997) 159-166.

[2] L.A. Utracki, Polymer Blends Handbook, Kluwer Academic Publishers, 2002.

[3] M. Cunha, S. Fakirov, Structure development during polymer processing, Kluwer Academic Publishers, 2000.

[4] M. Bilewicz, J.C. Viana, A.M. Cunha, L.A. Dobrzański, Morphology diversity and mechanical response of injection moulded polymer nanocomposites and polymer-polymer composites, Journal of Achievements in Materials and Manufacturing Engineering 15 (2006) 159-165.

[5] G. Wróbel, Z. Rdzawski, G. Muzia, S. Pawlak, The application of transient thermography for the thermal characterisation of carbon fibre/epoxy composites, Journal of Achievements in Materials and Manufacturing Engineering 36/1 (2009) 49-56.

[6] B. Ziębowicz, M. Drak, L.A. Dobrzański, Corrosion resistance of the composite materials: nanocrystalline powder – polymer type in acid environment, Journal of Achievements in Materials and Manufacturing Engineering 36/2 (2009) 126-133.

[7] L.A. Dobrzański, A. Tomiczek, B. Tomiczek, A. Ślawska-Waniewska, O. Iesenchuk, Polymer matrix composite materials reinforced by Tb0.3Dy0.7Fe1.9 magnetostrictive particles, Journal of Achievements in Materials and Manufacturing Engineering 37/1 (2009) 16-23.

[8] C.E. Powell, G.W. Beall, Physical properties of polymer/clay nanocomposites, Solid State and Materials Science 10 (2006) 73-80.

[9] J.C. Viana, N. Billon A.M. Cunha, The Thermomechanical Environment and the Mechanical Properties of Injection Moldings, Polymer Engineering and Science 44/8 (2004) 1522-1533.

[10] M. Rojek, J. Stabik, The influence of X-rays on strength properties of polyester vascular system prosthesis, Journal of Achievements in Materials and Manufacturing Engineering 35/1 (2009) 47-54.

[11] L.A. Dobrzański, A. Grajcar, W. Borek, Microstructure evolution and phase composition of high-manganese austenitic steels, Journal of Achievements in Materials and Manufacturing Engineering 31/2 (2008) 218-225.

[12] G. Wróbel, J. Kaczmarczyk, J. Stabik, M. Rojek, Numerical models of polymeric composite to simulate fatigue and ageing processes, Journal of Achievements in Materials and Manufacturing Engineering 34/1 (2009) 31-38.

[13] A. Lijia, H. Dayong, J. Jing, Mechanical properties and miscibility of polyethersulfone/ phenoxy blends, Journal of Applied Polymer Science 59 (1996) 1843-1847.

[14] Z. Xie, J. Sheng, Z. Wan, Mechanical properties and morphology of polypropylene/polystyrene blends, Journal of Macromolecular Science-Physics B 40/2 (2001) 251-261.

[15] T. Wan, L. Chen, Y.C. Chua, Crystalline Morphology and Crystallization kinetics of Poly(ethylene terephthalate)/clay Nanocomposites, Journal of Applied Polymer Science 94 (2004) 1381-1388.

[16] S.S. Ray, M. Biswas, Preparation and evaluation of composites from montmorillonite and some heterocyclic polymers: 3.A water dispersible nanocomposite from pyrrole–montmorillonite polymerization system, Materials Research Bulletin 35 (1999) 1187-1194.

[17] A.S. Solis, I. Romero-Ibarra, M. Estrada, Mechanical and rheological studies on polyethylene terephthalate-montmorillonite nanocomposites, Polymer Engineering and Science 44 (2004) 1094-1102.

[18] G. Gorrasi, L. Tammaro, M. Tortora, V. Vittoria, D. Kaempfer, Transport properties of organic vapors in nanocomposites of isotactic polypropylene, Journal of Polymer Science, Part B: Polymer Physics 41/15 (2003) 1798-1805.

[19] Y. Kojima, A. Usuki, M. Kawasumi, Mechanical properties of nylon 6-clay hybrid, Journal Material Research 8/5 (1993) 1185-1189.

[20] Q. Zhang, Y. Wang, Q. Fu, Shear-Induced Change of Exfoliation and Orientation in Polypropylene/ Montmorillonite Nanocomposites, Journal of Polymer Science Part B: Polymer Physics 41 (2003) 1-10.

[21] A.J. Pennings, Lamellar and fibrillar crystallization of polymers, Die Makromolekulare Chemie Supplement 2 (1979) 99-142.